ICAS 2021 SHANGHAI
International Council of the Aeronautical Sciences
32nd Congress of the International Council of the Aeronautical Sciences
September 6-10, 2021
Pudong Shangri-La, Shanghai, China

A Simplified Model for the Simulation of Synergistic Air-Breathing Rocket Engine

Xuesen Yang, Qian Yang & Wei Dong

School of Mechanical Engineering, Shanghai Jiao Tong University, Shanghai, 200240, China

Abstract

A simplified model for the numerical simulation of a Synergistic Air-Breathing Rocket Engine together with its precooler has been proposed in the present investigation. A literature survey on the thermodynamic parameters highlighting the energy cycles at various stations of SABRE engine has been conducted. Altogether 43 groups of energy conservation equations, pressure balance equations and power balance equations have been solved using a nonlinear system solver integrated in commercial software MATLAB. In addition to the mass flow rate, temperature and pressure at each station, the pressure ratios of the air compressor and the helium compressor, the expansion ratios of the helium turbine and the hydrogen turbine have all been investigated numerically. Moreover, as the critical component of SABRE engine, the precooler with micro-tube structures has been modeled based on two-dimension spatial discretization, and the results have been presented in the form of matrices, which show the high performance of the precooler.

Keywords: SABRE engine; precooler; simplified model; micro-tube structures

1. Nomenclature

T	=	Temperature
P	=	Pressure
g	=	Residual
PR	=	Pressure ratio
k	=	Specific heat ratio
air	=	Air
He	=	Helium
ox	=	Oxygen
mix	=	Mixture
U	=	Overall heat transfer coefficient
A	=	Heat transfer area
C_m	=	Heat capacity
q	=	Heat flux

2. Introduction

Synergistic Air-Breathing Rocket Engine (SABRE) is a combined cycle engine, which was initially developed in the early of last 80's century when British engineers selected it as the power plant of SKYLON [1]. Integration of an air-breathing engine with a rocket engine is the fundamental feature of the SABRE engine.

The air-breathing engine offers higher specific impulse at low speed. However, its low thrust-to-weight ratio limits the Mach number range. The SABRE engine is designed to have a high thrust-to-weight ratio but moderate fuel consumption whilst switching to the rocket engine mode at Mach number 5 and altitude of 26 kilometers. SABRE engine is one of the major technology challenge standing in the way of hypersonic flight. The ability of compressor to handle high temperature inlet flows is seriously limited by the necessity to compress air prior to combustion. In order to use the

atmospheric oxygen at high pressure, SABRE engine cools the incoming airflow through a precooler [2], which brings in a series of complications for the engine design, such as the fabrication of microtubes and its implementation. Moreover, the frost formed on the cooling surfaces of precooler induces an additional thermal resistance and decreases the performance of precooler [3].

Webber et.al [4] compared SABRE engine with LACE engine (Liquid Air Cycle Engine) and the results showed that through entropy minimization, the SABRE made substantial gains in performance over the traditional LACE precooled engine. It was demonstrated that the precooler is the major source of thermodynamic irascibility within the engine cycle, and the entropy can be reduced by increasing the heat transfer coefficient on the air side. Fernández-Villacé et.al [5,6] presented a numerical model of SABRE engine during the entire air-breathing mode using the programming environment of EcosimPro based on ESPSS (European Space Propulsion System Simulation) set of libraries, and a more realistic turbomachine behavior is implemented. The authors have proved the appropriateness for the simulation of SABRE engine during the air-breathing trajectory. Moral et.al [7] presented a simplified model using the standard ESPSS model of heat exchanger modules, and fitted the turbomachinery elements to represent the physical behavior of SABRE engine in design and off-design operation modes. Zhang et.al [8] carried out the efficiency calculation and cycle optimization for SABRE engine and proposed a method to improve the cycle efficiency. In this study, the cycle efficiency of SABRE engine is demonstrated to be between 29.7% and 41.7% within the entire flight envelope, and most of the wasted energy is occupied by the unburned hydrogen in exit gas.

Many studies to date have focused on the concept introduction of SABRE engine and qualitative analysis. Moreover, studies about engine performance mostly make use of commercial software. The main objective of the present investigation is to provide a simplified numerical code for simulation and optimization of SABRE engine including its precooler with easy approach. The code is programmed using MATLAB for its combination of concise language and portability.

3. Mathematical Model

3.1 Performance Model for SABRE Engine

The SABRE engine is designed to be capable of single-stage-to-orbit with two modes of operation, which is shown in Figure 1 and Figure 2. The air-breathing mode combines a turbo-compressor with a microchannel precooler just behind the intake, which chills the hot air, leading to an ultra-high pressure ratio. The high pressure air is subsequently fed into the rocket chamber where the air is ignited along with hot gas from the preburner. At the same time, part of the compressed air is fed into the preburner for the purpose of heating helium gas in the closed cycle. The valve located between the preburner and the turbo-compressor regulates the exhaust gas temperature, the heat transfers across the reheater and the helium turbine inlet temperature.

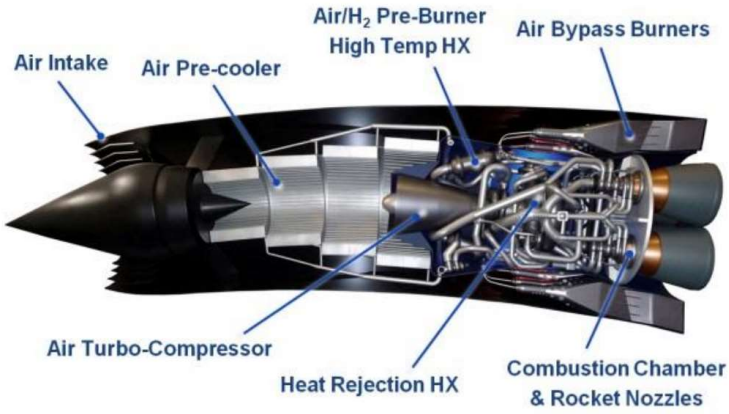

Figure 1 – SABRE engine. [9]

The air compressor is driven by helium turbine, and the temperature as well as the pressure of helium gas decrease at the same time. However, the temperature of helium is still very high and the heat is transferred into liquid hydrogen within HX4. The helium compressor driven by hydrogen turbine is used to compress the cooled helium gas to the previous pressure. At this moment, the closed helium loop is completed, and the supercritical helium gas is ready to chill the hot air from the intake.

On the other hand, liquid hydrogen is heated by hot helium gas and changes into hot hydrogen gas, which flows into hydrogen turbine and drives the helium compressor. Rich hydrogen gas flows into the preburner where it is ignited along with air to produce hot gas. Finally, the rich fuel gas flows into rocket chamber and joints the compressed air. Helium gas works as the intermediate medium and transfers heat from air to hydrogen though a closed cycle with constant mass. Although the nitrogen from the air cannot be used for participating in the combustion process, the thrust is increased when it flows through the nozzle at high speed. However, the equivalence ratio of air and hydrogen in the chamber cannot be 1 exactly since there is only about 23.3% oxygen in the air. According to the formula that describes the reaction process of air and hydrogen, when equivalence ratio is 2.8, remaining hydrogen will be wasted through nozzle [10]. Therefore, liquid oxygen is supplied into the system, which can be found in Figure 5, leading to difference in thrust and specific impulse compared with the key operating parameters of SABRE engine.

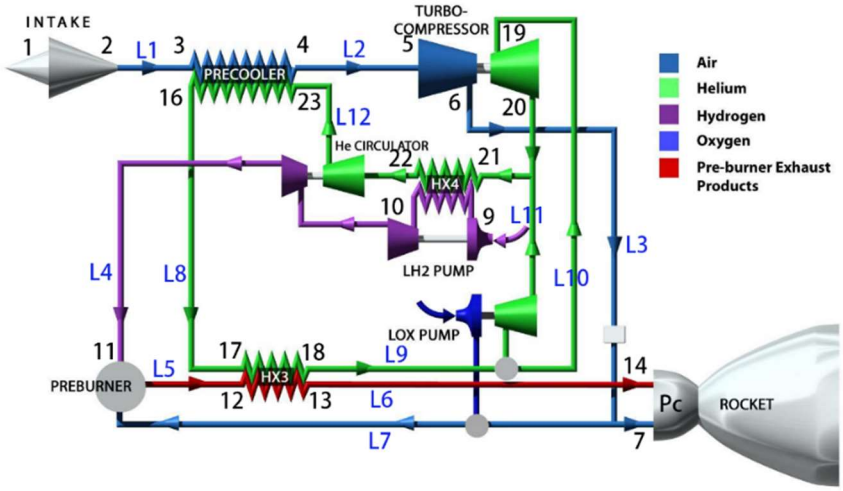

Figure 2 – Thermodynamic cycle of SABRE engine.

The thermodynamic cycle can be described as accurate math expressions in Table 1. The 43 groups of unknown variables needed to be solved, along with 43 groups of constraint equations. These 43 groups of variables consist of 1) temperatures and pressures at various stations; 2) pressure ratios of air compressor, helium turbine, helium compressor and hydrogen turbine; 3) mass flow rates of air, helium gas, liquid oxygen and liquid hydrogen. The 43 groups of constraint equations consist of energy conservation equations, power balance equations, and pressure balance equations.

Table 1 – Constraint equations.

Equation	No.	Equation	No.
$g_1 = T_4 - T_{4cal}$	(1)	$g_2 = T_{16} - T_{16cal}$	(2)
$g_3 = P_3 - P_4 - \Delta P_{4cal}$	(3)	$g_4 = P_{23} - P_{16} - \Delta P_{16cal}$	(4)
$g_5 = P_4 - P_5 - \Delta P_{L2}$	(5)	$g_6 = T_5 - T_4$	(6)
$g_7 = P_6 - P_5 * PR_1$	(7)	$g_8 = T_6 - T_5 \cdot PR_1{}^{((k-1)/k)}$	(8)
$g_9 = P_6 - P_7 - \Delta P_{L3}$	(9)	$g_{10} = T_7 - T_6$	(10)
$g_{11} = P_{fuel} - P_9$	(11)	$g_{12} = T_{fuel} - T_9$	(12)
$g_{13} = T_{22} - T_{22cal}$	(13)	$g_{14} = T_{10} - T_{10cal}$	(14)
$g_{15} = P_{21} - P_{22} - \Delta P_{22cal}$	(15)	$g_{16} = P_9 - P_{10} - \Delta P_{10cal}$	(16)
$g_{17} = P_{10}/P\,R_4 - P_{11} - \Delta P_{L4}$	(17)	$g_{18} = T_{11} - T_{10}/PR_4{}^{((k-1)/k)}$	(18)
$g_{19} = \left(P_{11} \cdot m_{fuel} + P_7 \cdot m_{air}/B\right)/m_{mix} - P_{12} - \Delta P_{L5}$	(19)	$g_{20} = T_{12} - T_f$	(20)
$g_{21} = T_{18} - T_{18cal}$	(21)	$g_{22} = T_{13} - T_{13cal}$	(22)
$g_{23} = P_{17} - P_{18} - \Delta P_{18cal}$	(23)	$g_{24} = P_{12} - P_{13} - \Delta P_{13cal}$	(24)
$g_{25} = P_{13} - P_{14} - \Delta P_{L6}$	(25)	$g_{26} = T_{14} - T_{13}$	(26)
$g_{27} = P_{16} - P_{17} - \Delta P_{L8}$	(27)	$g_{28} = T_{17} - T_{16}$	(28)
$g_{29} = P_{18} - P_{19} - \Delta P_{L9}$	(29)	$g_{30} = T_{19} - T_{18}$	(30)
$g_{31} = P_{20} - P_{19}/PR_2$	(31)	$g_{32} = T_{19} - T_{20} \cdot PR_2{}^{((k-1)/k)}$	(32)
$g_{33} = P_{20} - P_{21} - \Delta P_{L11}$	(33)	$g_{34} = T_{21} - T_{20}$	(34)
$g_{35} = P_{22} \cdot PR_3 - P_{23} - \Delta P_{L12}$	(35)	$g_{36} = T_{23} - T_{22} \cdot PR_3{}^{((k-1)/k)}$	(36)
$g_{37} = P_3 - P_2$	(37)	$g_{38} = T_3 - T_2$	(38)

$$g_{39} = P_{23} - P_{He} \quad (39) \qquad g_{40} = W_{5-6} - W_{19-20} \quad (40)$$
$$g_{41} = W_{10-11} - W_{22-23} \quad (41) \qquad g_{42} = P_7 - P_{13} \quad (42)$$
$$g_{43} = \dot{m}_{air} + \dot{m}_{fuel} + \dot{m}_{ox} - \dot{m}_{nozzle} \quad (43)$$

In the table, T_{cal} and ΔP_{cal} can be described as the functions of mass flow rate, pressure and temperature of heat transferring mediums, which can be described as follows.

$$\begin{aligned} T_{4cal}, T_{16cal}, \Delta P_{4cal}, \Delta P_{16cal} &= HX1(m_{air}, T_{air}, P_{air}, m_{He}, T_{He}, P_{He}) \\ T_{22cal}, T_{10cal}, \Delta P_{22cal}, \Delta P_{10cal} &= HX4(m_{He}, T_{21}, P_{21}, m_H, T_9, P_9) \\ T_{18cal}, T_{13cal}, \Delta P_{18cal}, \Delta P_{13cal} &= HX3(m_{mix}, T_{12}, P_{12}, m_H, T_{17}, P_{17}) \end{aligned} \quad (44)$$

Since the proposed model is zero-dimensional, coupling two-dimensional calculation of heat exchangers is not necessary. To perform rapid calculation of heat exchangers, the method developed by Kays and London [11], using the effectiveness-number of transfer units is used in the iterative process. In the sections of a precooler heat exchangers, the supercritical helium gas flows through the microchannel and are in cross flow with compressed air. The effective-NTU equations for unmixed cross flow heat exchangers can be given as

$$\varepsilon = 1 - \exp\left(1/C_m \cdot NTU^{0.22} \cdot (\exp(-C_m \cdot NTU^{0.78}) - 1)\right) \quad (45)$$

Assuming HX3 and HX4 are counter flow heat exchangers, the effectiveness can be given as

$$\varepsilon = \left(1 - \exp\left(-NTU \cdot (1 - C_m)\right)\right) \cdot \left(1 - C_m \cdot \exp\left(-NTU \cdot (1 - C_m)\right)\right) \quad (46)$$

where the number of transfer unit has the following value.

$$NTU = \frac{UA}{C_m} \quad (47)$$

3.2 Key Component Model for Precooler

NTU method is efficient in the simulation of SABRE engine, but a model with a higher precision is expected since the precooler is a key component. The configuration of the precooler is shown in Figure 3(a), and the precooler can be equalized as Figure 3(b).

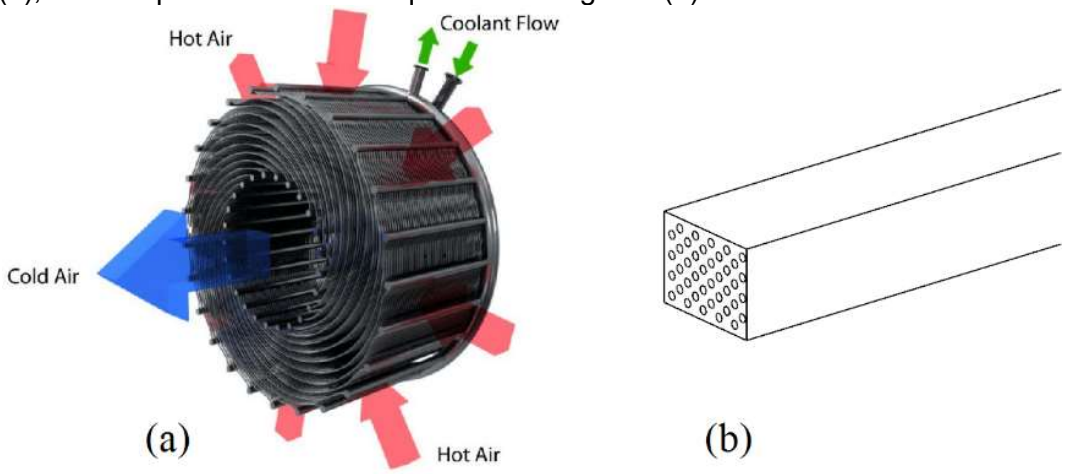

Figure 3 – The configuration and matrices module of SABRE engine. [3]

As shown in Figure 4, the precooler core is discretized into *i* × *j* micro units, where *i* is the layers of tubes and *j* is the number of cells along the direction of tubes. Apparently, the outlet condition of layer *i* is the inlet condition of layer *i*+1, and the outlet condition of cell *j* is the inlet condition of cell *j*+1. Within micro unit (*i*,*j*), we can build 4 groups of energy conservation equations that describe air, helium gas, hot side tube wall and cold side tube wall, respectively. Taking micro unit (*i*,*j*) as an example, heat fluxes in the hot channel are given by

$$q_1 = m_{i,j} h_{i,j} - \frac{kH_{i,j} A_h}{LH} \left(\frac{TH_{i,j} + TH_{i+1,j}}{2} - \frac{TH_{i,j} + TH_{i-1,j}}{2} \right) \quad (48)$$

$$q_2 = m_{i+1,j} h_{i+1,j} - \frac{kH_{i+1,j} A_h}{L_2} \left(\frac{TH_{i+1,j} + TH_{i+2,j}}{2} - \frac{TH_{i+1,j} + TH_{i,j}}{2} \right) \quad (49)$$

$$q_3 = \frac{NuH_{i,j} kH_{i,j}}{DH} A_{i,j} \left(\frac{TH_{i,j} + TH_{i+1,j}}{2} - TWH_{i,j} \right) \quad (50)$$

where $m_{i,j}$ is the mass flow rate; $A_{i,j}$ is the effective heat transfer area; A_h is the effective flow area of hot fluid; $h_{i,j}$ and $h_{i+1,j}$ are the enthalpies at inlet and outlet interfaces, respectively; $kH_{i,j}$ is the fluid thermal conductivity; LH is the characteristic length; $NuH_{i,j}$ is a function to calculate the local Nusselt number; $TWH_{i,j}$ is the wall temperature at the hot side. The heat transfers in the microtubes

are solved in an analogous way.

Heat conductions in the axial direction along the tube wall are calculated as

$$q_{71} = -\frac{kW \cdot A_w}{L/n}\left(\frac{TWH_{i,j}+THC_{i,j}}{2} - \frac{TWH_{i,j-1}+THC_{i,j-1}}{2}\right) \quad (51)$$

$$q_{72} = -\frac{kW \cdot A_w}{L/n}\left(\frac{TWH_{i,j+1}+THC_{i,j+1}}{2} - \frac{TWH_{i,j}+THC_{i,j}}{2}\right) \quad (52)$$

where q_{71} is the heat fluxes at the left side and q_{72} is the heat fluxes at the right side.

The cross wall heat fluxes are calculated as follows.

$$q_{7h} = \frac{kW \cdot A_w}{t}\left(TWH_{i,j} - THC_{i,j}\right) - \frac{q_{71}-q_{72}}{2} \quad (53)$$

$$q_{7c} = \frac{kW \cdot A_w}{t}\left(TWH_{i,j} - THC_{i,j}\right) + \frac{q_{71}-q_{72}}{2} \quad (54)$$

The actual temperatures are solved by using these relationships to minimize the residuals of energy conservation equations:

$$\begin{aligned} 0 &= q_1 - q_2 - q_3 \\ 0 &= q_3 - q_{7\mathrm{h}} \\ 0 &= q_4 - q_{7\mathrm{c}} \\ 0 &= q_4 + q_5 - q_6 \end{aligned} \quad (55)$$

Eq. (55) can be solved using a system solver integrated in MATLAB, namely '*fsolve*'.

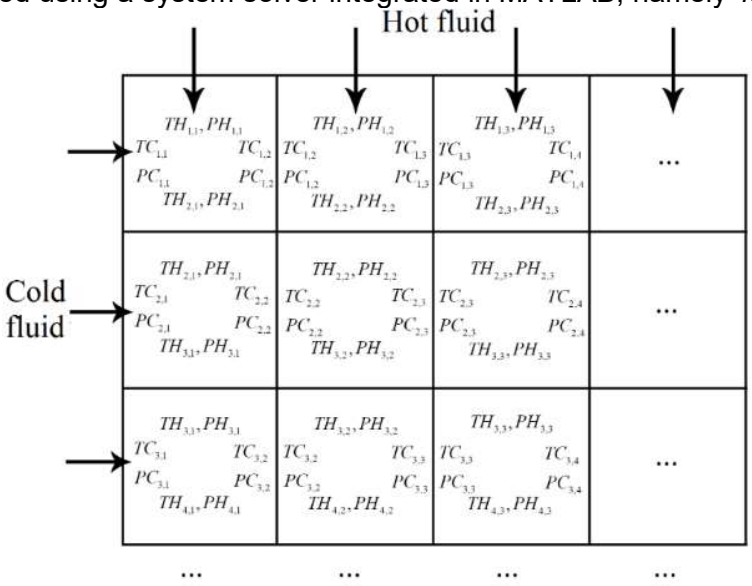

Figure 4 – Spatial discretization of matrices module.

Heat transfers are determined by empirical heat transfer correlations that take account of the local flow conditions and thermal properties. Murray et.al [12] built and tested a small precooler heat exchanger with 0.38 mm tubes using conditions reflecting the operating characteristics of the helium flight precooler of the SABRE engine, and gave a correlation with the bulk Reynolds number by fitting a curve to the interpolated data for external flow as follows.

$$St = \frac{h}{Gc_p} = 0.5978\mathrm{Re}^{-0.39}, \mathrm{Re} < 3000 \quad (56)$$

The friction factor was also given in an analogous way, which allows to determine the pressure drop from one cell to the next using the following empirical correlations:

$$\frac{1}{4}f_{Darcy} = 0.1923\left[\frac{\mathrm{Re}}{3000}\right]^{-0.04}, \mathrm{Re} < 3000 \quad (57)$$

Murray et.al [12] demonstrated that the relations are with the best fit accuracy of approximately 3% in the range of Re<3000.

The internal flow has been well researched in previous work, and the Nusselt number is calculated according to the correlations of Taylor [13].

$$Nu = 0.023\mathrm{Re}^{0.8}\mathrm{Pr}^{0.4}\left(\frac{T_S}{T}\right) \cdot \exp\left(-\left(0.57 - \frac{1.59}{\frac{x}{D}}\right)\right) \quad (58)$$

And the friction factor is given according to Haaland equation [14].

$$f_{Darcy} = \left(-1.8\lg\left(\left(\frac{\varepsilon}{3.7D}\right)^{1.11} + \frac{6.9}{\mathrm{Re}}\right)\right)^{-2} \quad (59)$$

where f_{Darcy} is the Darcy friction factor; ε is the tube roughness height; D is the tube diameter.

4. Results and discussion

4.1 Performance Discussion

Since some of the key parameters of SABRE engine are confidential, the related data are gathered from different publications and the heat exchangers parameters are adjusted to allow a direct calculation. For this reason, verifying the model itself becomes the focus of this study rather than the precision of the results compared with the actual performance of the SABRE engine. Table 2 gives the key operating parameters of SABRE engine.

Table 2 – Key operating parameters of SABRE engine.

Air-breathing Mode		Rocket Mode	
Altitude	20270 m	Hydrogen Mass Flow	46 kg/s
Mach No.	4	LOX Mass Flow	278 kg/s
Intake Pressure Recovery Factor	0.1592	Chamber Pressure (nominal)	145 bar
Hydrogen Mass Flow	31 kg/s	Total Thrust	145.8 ton
Equivalence Ratio	2.8		
Air Mass Flow	382 kg/s		
Chamber Pressure (nominal)	103.8 bar		
Core Engine Gross Thrust	104.5 ton		
Total Gross Thrust (including By-Pass Flow)	145.0 ton		

Figure 5 gives the simulation results of SABRE engine at Mach number 4, height 25 kilometers, operating in air-breathing mode. However, the air must be decelerated since the pressure drop of air gets large rapidly with the increasing Mach number. The total pressure and temperature of the air are 322 kPa and 924.8 K, respectively, before flowing into the precooler. Subsequently, the air is chilled down to 199.7K under fixed pressure by helium gas at 134.8 K. The pressure ratio of air turbo-compressor is 66, which could even reach 150 under certain circumstances if the inlet pressure of precooler is much smaller or the pressure drop is much larger to keep the pressures of air and hydrogen balanced. The compressed air at temperature 662.8 K and pressure 21.24 MPa is used to supply the rocket combustion chamber and preburner.

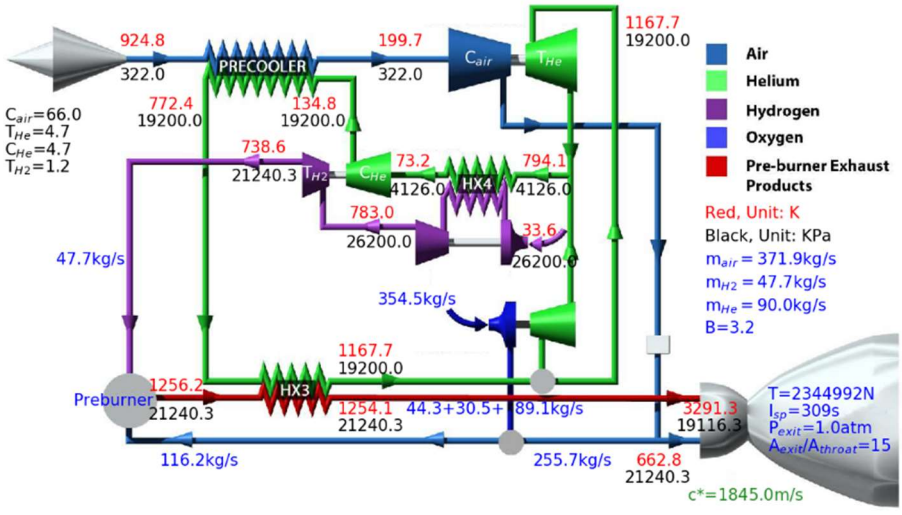

Figure 5 – Simulation results at different positions (Ma=5, H=25km).

On the other hand, the hot helium gas with a temperature of 772.4 K is heated up again by an auxiliary heat exchanger to 1167.7 K under fixed pressure. The hot helium gas drives turbine to work and the expansion ratio is 4.7, which indicates that the fluid used to heat up hydrogen is at the temperature of 794.1 K and pressure of 4.126 MPa. Meanwhile the exit temperature of helium gas is 73.2 K, which increases to 134.8 K after being compressed by the helium turbine. Liquid hydrogen is heated up to 783 K and is able to drive the hydrogen turbine. The combustion chamber temperature is 3291.3 K which is determined by energy conservation equations. Applying the nozzle characteristics, it is easy to find that the gross thrust is 234.5 ton and the specific impulse is 309 s.

Figure 6 shows the residuals of these 43 groups of equations in Table 1, and the least residual is smaller than 10^{-8} after 264 iterations while the initial residuals are huge.

To investigate how the performance changes under various conditions, we first performed simulations with the temperature in the range of 300 K to 1600 K, then with the pressure in the range of 1 atm to 20 atm, and at last with a given flight mission. The performance parameters to be evaluated are thrust, specific impulse, pressure ratio, critical temperature and mass flow rate. Moreover, the mass flow rates of helium gas and liquid hydrogen maintain constant.

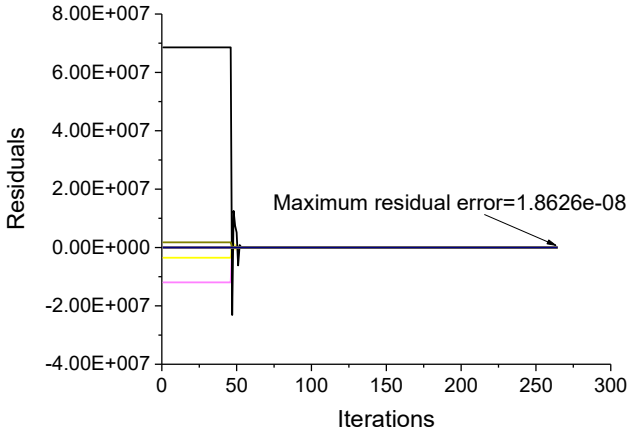

Figure 6 – Residuals of 43 groups of variables during iterative process.

4.2 Precooler performance discussion

Considerable literature mentioned a precooler core named JMHX of SABRE engine, which consists of 415 microtubes packed in 38.95 mm × 40 mm × 3.762 mm. The tube inner diameter of JMHX is 0.28 mm, when the actual tube inner diameter of SABRE engine is 0.9 mm. Moreover, nitrogen gas with a temperature of 80 K is used as the coolant to chill nitrogen gas with a temperature of 1000 K, when the actual working fluids are helium gas and air, respectively. In the present study, we use the actual tube diameters and actual working fluids to study the precooler performance of SABRE engine, at the same boundary conditions for comparison, which is shown in Table 3. It can be seen that the total mass flow rates of helium gas and air are both 0.023 kg/s.

Table 3 – Boundary conditions.

T_{cin}	80 K	P_{cin}	10 MPa	m_{cin}	0.023 kg/s
T_{hin}	1000 K	P_{hin}	100 kPa	m_{hin}	0.023 kg/s

For this case, the precooler module has 10 layers with alternating layers of 41 and 42 tubes. In other words, there are 41.5 tubes on average. Therefore, if we discrete n grids in the direction of tubes, the inlet mass flow rate of air is (0.023/41.5/n) kg/s, when the inlet mass flow rate of helium is always (0.023/415) kg/s. A total of 10n micro units bring 4×10n equations to solve. The computational cost will increase with more layers and grids. If we calculate the full-scale precooler, which means tens of millions of equations are to be solved simultaneously. One of the solutions is space stepping method. Since the air flows through the microtubes one layer by one layer, we can solve at most 4n equations at the same time. Then the inlet condition of next layer will be the outlet condition of previous layer, which has already been solved.

Depending on the mathematical model of the precooler proposed in this study, it is able to calculate the temperature and pressure of every micro unit, and the results are shown in Figure 7. The total heat transfer power is 11.6 kW and the average outlet temperature of air and helium are 538.5 K and 175.4 K, respectively.

Obviously, the layers of microchannel should be increased since the designed outlet temperature of air for the precooler is 123.15 K. Figure 8 gives the results when the layers of microchannel add up to 56 and the total heat transfer power is 21.12 kW. Figure 9 and Figure 10 describe the outlet temperatures of helium and air, respectively. It can be seen that the minimum temperature of air is 122.8 K while the maximum temperature of air is 134.1 K, therefore the differential temperature is only 9.2 percent of the minimum temperature. It is worth noting that the friction factor of air is almost 30 times of those of helium, which denotes a larger pressure loss of air. It can also be found that the non-uniformity of temperature decreases with the increasing number of layers.

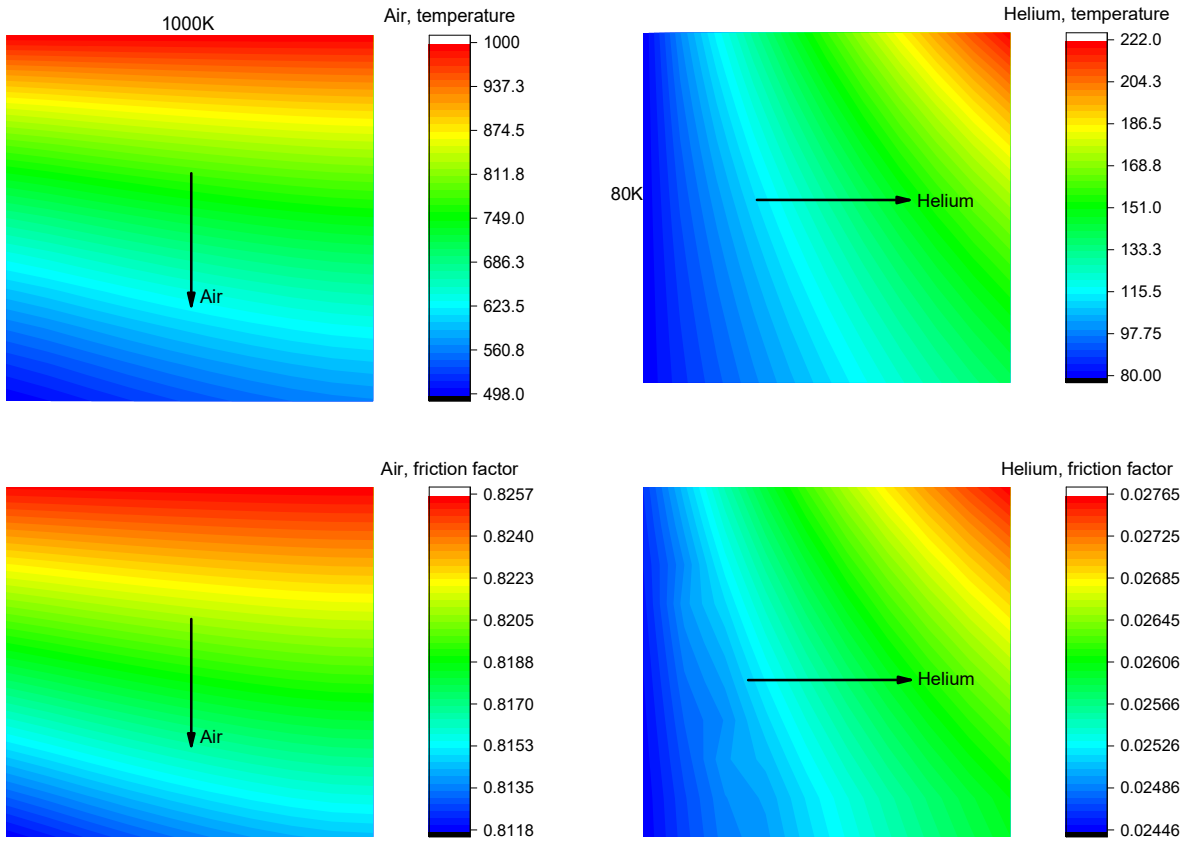

Figure 7 – Performance of precooler core (black arrows indicate the flow directions).

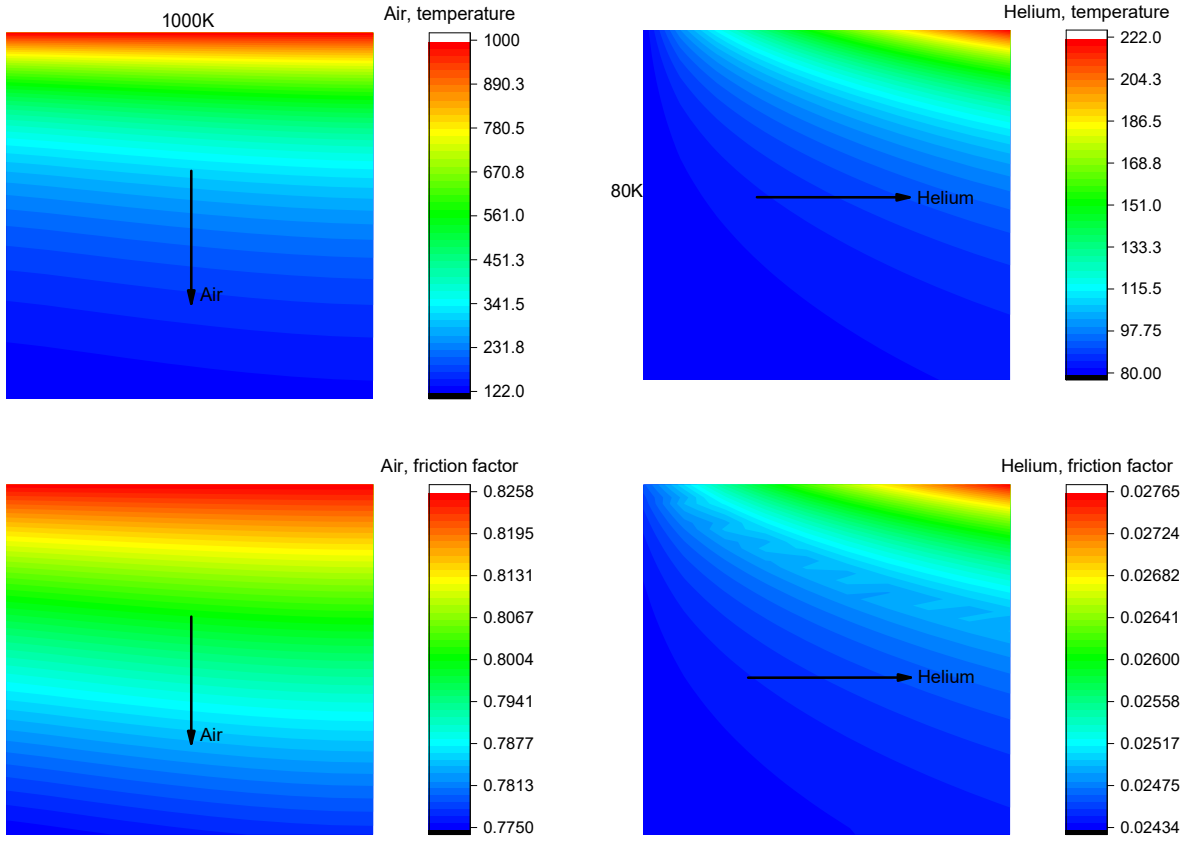

Figure 8 – Performance of precooler core when the outlet temperature of air reaches 150°C.

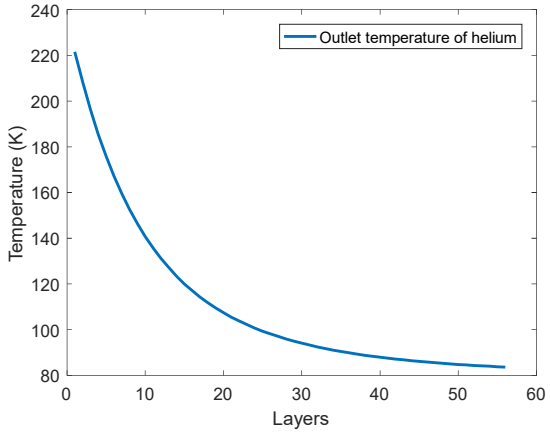

Figure 9 – Outlet temperature of helium.

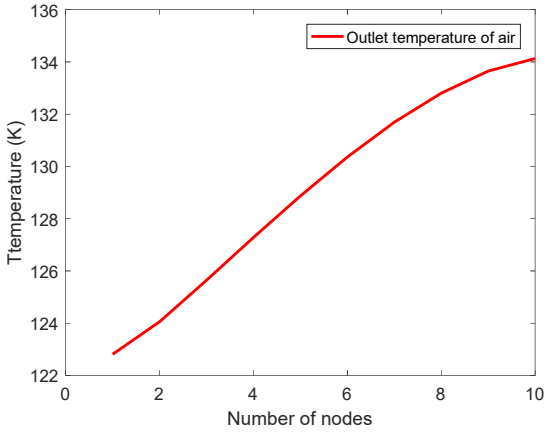

Figure 10 – Outlet temperature of air.

5. Conclusions

A simplified model for the steady simulation of Synergistic Air-Breathing Rocket Engine has been proposed and implemented using commercial software MATLAB. Temperature, pressure ratio, heat transfer efficiency and mass flow rate at various stations are considered in the governing equations of the model according to the real thermal cycle processes. The inputs of the SABRE engine simulation program include the flight Mach number, flight height, bypass ratio, mass flow rate of helium, mass flow rate of liquid hydrogen, geometry parameters of heat exchangers, geometry parameters of nozzle and the thermodynamic parameters. The outputs are the pneumatic parameters at various stations and the corresponding performance of the SABRE engine. The results of the simulation model are compared and checked with the available data in open literature regarding to the SABRE engine. Moreover, as the key component, the performance of the precooler has also been analyzed with a 2D model considering energy balance and pressure balance. For this geometry structure, 56 layers of microchannel are found to be enough to cool the air from 1000 K to 123.15 K.

6. Copyright Statement

References

[1] Varvill R and Bond A. The Skylon spaceplane: progress to realisation. Journal of the British Interplanetary Society, Vol. 61, No. 10, pp 412-418, 2008.

[2] Jivraj F, Bond A, Varvill R and Paniagua G. The scimitar precooled Mach 5 engine. 2nd European conference for aerospace sciences (EUCASS), Belgium, pp 1-10, 2007.

[3] Jian D and Qiuru Z. Key technologies for thermodynamic cycle of precooled engines: A review. Acta Astronautica, Vol. 177, pp 299-312, 2020.

[4] Webber H, Bond A and Hempsell M. The sensitivity of precooled air-breathing engine performance to heat exchanger design parameters. JBIS - Journal of the British Interplanetary Society, Vol. 60, pp 188-196, 2007.

[5] Fernández-Villacé V and Paniagua G. Simulation of a Combined Cycle for High Speed Propulsion. 48th AIAA Aerospace Sciences Meeting Including the New Horizons Forum and Aerospace Exposition, AIAA 2020-1125, USA, 2010.

[6] Fernández-Villacé V. Simulation. Design and Analysis of Air-Breathing Combined-Cycle Engines for High Speed Propulsion. Doctoral Thesis, Von Karman Institute for Fluid Dynamics, 2013.

[7] Moral J, Vilá J, Di Matteo F and Steelant J. ESPSS Model of a Simplified Combined-Cycle Engine for Supersonic Cruise. Proceedings of Space Propulsion, Italy, 2016.

[8] Zhang J, Wang Z and Li Q. Thermodynamic efficiency analysis and cycle optimization of deeply precooled combined cycle engine in the air-breathing mode. Acta Astronautica, Vol. 138, pp 394-406, 2017.

[9] Hempsell M. Progress on the SKYLON and SABRE. Proceedings of the International Astronautical Congress, China, pp. 8427-8440, 2013.

[10] Petrescu RV, Aversa R, Akash B, Bucinell, R, Corchado J, Apicella A and Petrescu FI. Modern propulsions for aerospace-a review. Journal of Aircraft and Spacecraft Technology, Vol. 1, 2017.

[11] Zohuri B. Compact heat exchangers. 1nd edition, Springer, 2017.

[12] Murray JJ, Hempsell CM and Bond A. An experimental precooler for airbreathing rocket engines. JBIS - Journal of the British Interplanetary Society, Vol. 54, pp 199-209, 2001.

[13] Taylor MF. Correlation of Local Heat-Transfer Coefficients for Single-Phase Turbulent Flow of Hydrogen in Tubes With Temperature Ratios To 23.National Aeronautics and Space Administration, 1968.

[14] Haaland SE. Simple and Explicit Formulas for the Friction Factor in Turbulent Pipe Flow. Journal of Fluids Engineering, Vol. 105, pp 89, 1983.